Reactive oxygen species induced by water containing nano-bubbles and its role in the improvement of barley seed germination

Shu LIU[1], Seiichi OSHITA[1,*], Yoshio MAKINO[1]

* Corresponding author: Tel.: ++81 03 58415362; Fax: ++81 (0)1895 256392; Email: aoshita@mail.ecc.u-tokyo.ac.jp
1 Graduate School of Agricultural & Life Sciences, The University of Tokyo, Japan

Abstract The study of reactive oxygen species (ROS) generation caused by nano-bubbles (NBs) is of great importance for its application in both physiological activity promotion aspect and sterilization aspect. In this paper, Aminophenyl Fluorescein (APF) was used as a fluorescent reagent for the detection of ROS generation by NBs. The NBs scattering could cause the decrease of fluorescence intensity. Meanwhile, the quenching effect of oxygen could also cause the decrease of fluorescence intensity. Although the above two factors masked the fluorescence intensity generation by ROS, the fluorescence intensity of the water containing NBs still increased with NBs generation time, which proved that oxygen NBs could generate ROS. Moreover, the endogenous ROS in the barley seed cells were measured in the seed that germinated in the water containing NBs and the distilled water respectively. According to the results of seed staining experiments, both the microscope images and the absorbance at 560nm proved that the seeds dipped in the water containing NBs could generate more ROS compared to those in the distilled water. These findings greatly increase the NBs potential use both in agricultural field and environmental field.

Keywords: Bubble size distribution, Hydroxyl radicals, APF, Bubble scattering, Microscope spectrophotometer

1. Introduction

Bulk nano-bubbles (NBs) are an upcoming field with a lot of unknown questions. In recent years, NBs' physiological activity promotion effect and sterilization effect have both been reported. It has been proved that the water containing NBs can accelerate the growth of plants, shellfish and yeast (Ebina et al. 2013). Park and Kurata (2009) found that fresh weights of microbubble-treated lettuces were 2.1 times greater than those of the macrobubble-treated lettuces, when grown under a similar dissolved oxygen (DO) concentration. Liu et al. (2013) reported that the germination rates of barley seeds dipped in water containing NBs were 15–25 percentage points greater than those of the seed dipped in distilled water with the same concentration of DO.

On the other hand, a series of articles from the research group of Takahashi reported that free radicals are generated by the collapse of microbubbles (MBs) in the absence of dynamic stimulus, such as ozone (Takahashi et al. 2012), strong acid (Takahashi et al. 2007) and copper (Li et al. 2009). The ozone micro and nanobubbles (MNBs) can greatly enhance the ozonation process compared to the conventional ozone bubbles contactor (Takahashi et al. 2012; Chu et al. 2008; Ikeura et al. 2011). Apart from the absence of dynamic stimulus, air MNBs itself can be used to detach the biofilm and clean the oil pipe (Hiroyuki et al. 2010; Agrwal et al. 2012).

The physiological promotion and sterilization described above may seem contradictory to each other. However, the generation of reactive oxygen species (ROS) caused by NBs could offer a reasonable explanation for the above two NBs' effects. ROS played a vital role in the growth by facilitating the required cell wall loosening for cell elongation (Passardi et al. 2004). Meanwhile, it has been reported that the reactive oxygen species, such as hydrogen

peroxide, enhanced germination and released residual dormancy of barley seeds (Mabuchi, 1994; Ishibashi et al. 2010). Also, hydroxyl radical was generated in the cell wall during radicle elongation and weakening of endosperm of cress seeds (Muller et al. 2009). On the other hand, ROS are capable of causing oxidative damage to macromolecules, thus leading to lipid peroxidation, DNA damage, and DNA breaks (Tomizawa et al. 2005). Owing to the above principles they are widely used in sterilization process. In sterilization and oxidation aspects, sufficient amount of ROS was needed for practical applications. While, in biological field, appropriate amount of ROS would promote the physiological activity of living organisms. On the contrary, overproduction of ROS might become deleterious. With this idea in mind, we have studied the generation of ROS by NBs using a novel fluorescent reagent Aminophenyl Fluorescein (APF) and estimated the oxidative capacity of NBs. To further confirm the stimulation effect of NBs on the generation of ROS in living organisms, we also studied the ROS generation in the germinated barley seed both in the water with and without NBs.

2. Materials and methods

2.1 Generation of ROS by NBs

2.1.1 Reagents

Aminophenyl Fluorescein (APF) (Sekisui Medical CO., LTD.) was used as a fluorescent reagent for the detection of ROS generation by nano-bubbles (NBs). APF itself has almost non-florescent intensity. After APF reacts with ROS, a fluorescein with strong fluorescent intensity will generate. Many ROS have very short lifetimes, such as 1×10^{-9}s for ·OH (Donoghue et al. 2013), in the range of milliseconds to seconds at neutral pH values for $O_2^{\cdot-}$ (Chen et al., 2008). Thus, sensitive and fast-response detection methods are needed to quantify the ROS concentrations in NBs water. APF as a fluorescent probe was highly resistant to autoxidation (Setsukinai et al. 2003). As a result, it is very appropriate in our experiments. Other chemicals were purchased from Kanto Chemical Co., Inc. and were of the highest obtained purity. Hydrogen peroxide and ferrous sulfate were prepared each time they were to be used.

2.1.2 Experimental procedures

As for the first method, 5 mM APF reagent was diluted with phosphate buffer (0.1M, pH 7.4). The buffer was made from ultrapure water. Then MNBs were introduced into the 500mL APF solution through a micro-bubble generator (OM4-GP-040, Aura Tec Co. Ltd., Japan) at a constant temperature of 20℃ to verify the production of hydroxyl radicals. After 10 minutes, 30 minutes and 60 minutes generation time, the samples of 10mL were taken for the fluorescent intensity measurement. For the second method, NBs were generated in 500mL phosphate buffer without APF for 10 minutes, 30 minutes and 60 minutes, respectively. Then APF was added in the buffer containing NBs, and the fluorescent intensities of samples were measured. The same concentration of APF (1μM) was applied in both two methods.

2.1.3 Fluoremetric analysis

The fluorescence intensities were measured at excitation wavelength of 490nm and fluorescence emission wavelength of 515nm with a fluorescence spectrophotometer (F-7000, Hitachi High-Tech Co. Ltd., Japan). The slit width was 5nm for both excitation and emission. The photomultiplier voltage was 700 V.

2.1.4 DO concentration and pH

Dissolved oxygen (DO) concentration was measured in both control water and water containing NBs at 20℃ using a DO metre (SG6, Mettler Toledo GmbH, Switzerland). The pH was measured by a pH meter (D-55, Horiba Ltd., Japan). The measurement range of this pH meter is from 0 to 14 with accuracy of ±0.01. The pH meter was set to compensate automatically the pH value at 20 ^{o}C.

2.1.5 Bubble-size distribution

Bubble-size distributions were measured using the dynamic light scattering method (NanoSight-LM10, Quantum Design Inc., Japan). Using a laser-illuminated optical

microscope, we observed NBs as light-scattering centres moving under Brownian motion. After NBs were generated for 10 minutes, 30 minutes and 60minutes, they were in the BOD bottles for about 1 hour to stabilize. Bubble-size distribution was measured as a function of generation time. The bubbles were formed with oxygen.

2.2 Generation of ROS in seeds

2.2.1 Seed germination

Barley seeds (*Hordeumvulgare* L.) were harvested in 2011 and were obtained from the University of Ehime, Japan. Germination tests were performed with a pair of seed groups composed of 100 barley seeds each. One group was dipped in a 1-L beaker filled with distilled water containing NBs and the other in a beaker filled with distilled water. The DO concentrations of NBs water and the distilled water were adjusted to be the same. The preparation of water containing NBs and control was the same with our previous paper (Liu et al. 2013). Germination temperature was maintained at 20 ℃ with a water bath.

2.2.2 Amount of ROS in seeds

After 22 hour and 50 hours dipping time, 3 geminated seeds in each group were incubated in 2mM nitroblue tetrazolium (NBT) in 10mM Tris-HCl buffer (pH 7.34) at room temperature for 30 minutes. Then the seeds were cut vertically into 100μm slices continuously from the tip of sprout part with a cutting machine (Leica CM1950, Leica Biosystems Co. Ltd., Japan). ROS (superoxide radical) can be visualized as deposits of dark-blue insoluble formazan compound using microscope spectrophotometer (MSV-5000, JASCO Co. Ltd., Japan). After 22 hours' dipping time, the sprouts were cut into four samples. While after 50 hours' dipping time, the grown-up sprouts were cut into eight samples. For each sample, 5-12 measurement dots were selected. The diameter of each measurement dots was 10μm. The average absorbance values were used to represent the relative amount of ROS in each seed.

3 Results and discussions

3.1 Production of hydroxyl radicals by NBs

3.1.1 Production of ROS during the MNBs' generation in the buffer solution

Fig. 1 shows the excitation emission matrix of fluorescence (EEM) spectra of APF solution before and after oxygen MNBs generation (Figs. 1A and 1B). The fluorescent intensity was determined at 515 nm with excitation at 490 nm. APF was added in the phosphate buffer solution before MNBs generation started. Fig. 1C showed the change of fluorescent intensity of APF solution (control) and the change of which with MNBs at different generation time. The horizontal axis shows the time of measurement point.During the bubble generation, both NBs and MBs were formed. Here we use the expression of 'MNBs' in this part.

As evident in Fig. 1, at the same measurement time, the fluorescent intensities

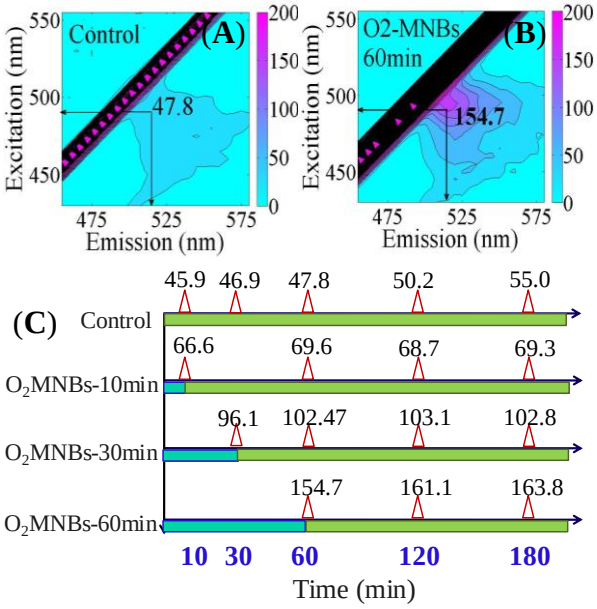

Fig.1 The fluorescent intensity of APF solution before and after oxygen MNBs generation (A: the EEM spectra of APF solution; B: the EEM spectra of APF solution after 60 minutes generation; C: the change of fluorescent intensity of APF solution (control) and the change of which with MNBs at different generation time. The solid bars show the MNBs generation time. The white bars show the sample storage time. The values in Fig 1(C) represent the fluorescent intensities at 515nm with excitation at 490nm. DO concentration of these oxygen NBs water were above 40mg/L; APF concentration 1μM)

of MNBs solutions were significantly stronger than those of control water. The above results proved that oxygen MNBs could generate ROS in the water. The fluorescent intensity in the APF solution increased gradually with oxygen MNBs generation time. For nitrogen MNBs, the fluorescent intensity didn't remarkably change with MNBs generation time (data not shown), which meant the amount of ROS generated by nitrogen MNBs was too small to be detected.

3.1.2 Production of ROS after MNBs' generation in buffer solution

For the sake of studying the generation of ROS by NBs, APF was added after MNBs solution became clear, which meant only NBs were left in the solution. Here in this part, the expression of 'NBs' is used.

As can be seen in Fig. 2, the fluorescent intensity in the APF solution also increased with different oxygen NBs generation time. However, compared to the first method, the fluorescence increase was less obvious. Hydroxyl radicals are highly reactive and consequently short-lived. Therefore, more fluorescein can be produced during the MNBs generation. Bubble-number density increased with longer generation times, which was supported by the results shown in Fig. 3. The geometric mean bubble size observed was around 130 nm. The bubble number density corresponded to the fluorescent intensities in Fig. 1 and Fig.2. Thus, we can conclude that the amount of ROS has positive correlation with the number of oxygen NBs in the water. According to Li et al. (2009), hydroxyl radicals formed by collapsing MBs in aqueous solution. And the results here proved that oxygen NBs can also generate ROS in the water.

3.2 Quenching of fluorescence

The first-order scattering line was due to three kinds of scattering: Rayleigh scattering, Tyndall scattering and scattering from the cuvette surface. When the water contains a large amount of NBs, a scattered beam can be observed due to Tyndall effect caused by NBs (Najafi et al. 2007). NBs are inherently hydrophobic (Seddon et al. 2012), which will drive them to adhere to the glass wall causing cuvette surface scattering. MNBs scatter both excitation and emission light and thus reduce the detected fluorescence intensity (Kopechek et al. 2013). The reduction in fluorescent intensity was reasonably expected. Therefore the scattered effect was measured as shown in Fig. 4.

Fig. 4 shows the intensities of first-order scattered light in the APF solution with and without MNBs. The representative point (Ex=Em=500nm) was used to show the intensity of first-order scattered light. As can be seen in Fig. 4, the scattering intensities of APF solution containing NBs were more than 8 times stronger than those without NBs. There was a larger amount of fluorescein produced by APF in the oxygen NBs water, and fluorescein molecules themselves led to

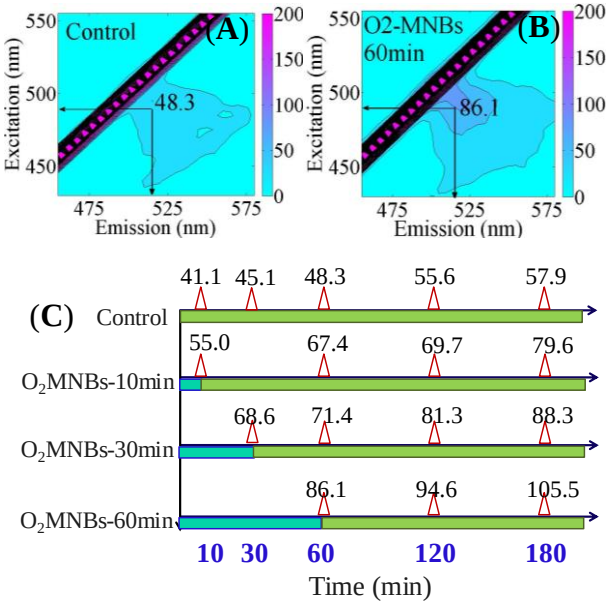

Fig. 2 The fluorescent intensity of APF solution with and without oxygen NBs (A: the EEM spectra of APF solution; B: the EEM spectra of APF solution with oxygen NBs and the generation time of which is 60 minutes; C: the change of fluorescent intensity of APF solution without (control) and with oxygen NBs with different time of occurrence. The blue bars show the MNBs generation time. The green bars show the sample storage time. The values in Fig 1(C) represent the fluorescent intensities at 515nm with excitation at 490nm. DO concentration of these oxygen NBs water were above 40mg/L; APF concentration 1μM)

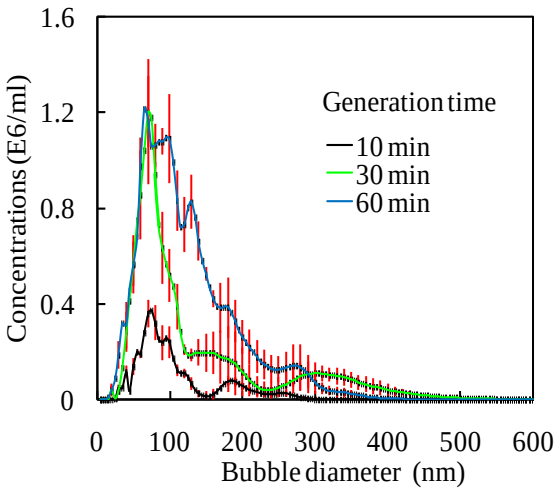

Fig. 3 Bubble size distribution in the water containing oxygen NBs with different generation times.(Red error bars indicate standard error of the mean (n=3))

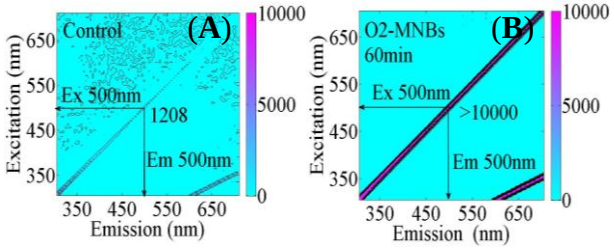

Fig. 4 Fluorescence intensity on the scattering line of different kinds of NBs water. (Oxygen NBs (B) were produced from control water (A), Then representative point (Ex=Em=500nm) was used to show the intensity of first-order scattered light; DO concentration of oxygen NBs water were 40mg/L; NBs generation time was 60 minutes; APF 1μM)

the stronger scattering intensity in the oxygen NBs water.

Molecular oxygen is a best-known collisional quencher, which quenches almost all known fluorophores (Lakowicz and Weber, 1973). In NBs system, the DO concentration of NBs water and the buffer solution were of huge difference. Therefore in the study of ROS produced by NBs, the reduction in fluorescence caused by oxygen must also be considered in the future.

3.3 Estimation the oxidative capacity of NBs

We have provided the direct evidence that oxygen NBs can generate ROS, while we are also interested in the question of how much amount of ROS can be generated in the oxygen NBs water. H_2O_2 was added in the phosphate buffer solution of APF and then ferrous sulfate was added. As can be seen in Fig. 5, ·OH which formed in the Fenton reaction was detected using APF. Ferrous iron (II) is oxidized by hydrogen peroxide to ferric iron (III), a hydroxyl radical, and a hydroxyl anion. The concentration of ferrous iron is equal to the concentration of hydroxyl radicals. The fluorescence increase was proportional to the concentration of H_2O_2. According to Setsukinai's research (2003), APF showed fluorescence augmentation only upon ·OH and –OCl, but not upon other kinds of ROS. Fig. 6 showed that APF can be used to detect the existence of H_2O_2 in terms of a dose-dependent increase of fluorescence at the range of low H_2O_2 concentrations. The results from Fig. 5 and Fig. 6 showed that H_2O_2 can produce very small amount of ·OH compared to the Fenton reaction. When the similar fluorescent intensities were produced in the APF solution, the concentration of H_2O_2 was about 1000-fold more than that of ferrous. So the data agreed well with Setsukinai et al. (2003) and Donoghue et al. (2013). ·OH can also be produced during dissociation of H_2O_2 by UV-light. The EEM spectra were collected with corresponding scanning emission spectra from 300 nm to 700 nm at 5 nm increments by

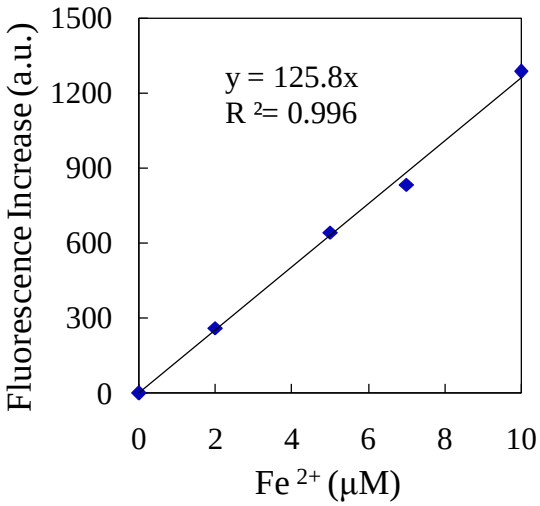

Fig. 5 Detection of ·OH in the Fenton reaction using APF. (In the horizontal axis, the concentration of Ferrous iron (II) is equal to that of hydroxyl radicals; 1μM APF was added in the phosphate buffer (0.1M, pH 7.4) containing H_2O_2 (0.4mM). The fluorescence intensity was determined at 515nm with excitation at 490nm.)

varying the excitation wavelength from 300 nm to 700 nm at 5 nm sampling intervals. As a result, there exists a possible reason that, during the fluorescence measurement, a small amount of ·OH will generate from the decomposition of H_2O_2.

According to the data from Fig. 5 and Fig.6, the fluorescence increase in the APF solution caused by 60 minutes oxygen MNBs generation was calculated, which was about 107 (Fig. 1). According to the formula in Fig. 5 and Fig. 6, the fluorescence increase was equivalent to 0.85μM ·OH or 1.5 mM H_2O_2. The reduction in florescence caused both by oxygen and light scattering from bubbles being considered, the oxidative capacity of 60 minutes generation of oxygen NBs should be originally higher than 0.85μM ·OH or 1.5 mM H_2O_2. Our results, to our knowledge, are the first to be used to quantify the oxidative capacity of oxygen MNBs in the water. The generation of ROS by NBs could play a positive role both in the defense system of plants against pathogenic organisms and promotion of physiological activity of plants.

3.4 The stimulating effect of NBs on the ROS inside barley seed

Comparison germination tests were performed using distilled water and water containing NBs under the similar dissolved oxygen concentrations. After 22 hours' dipping time, the germination rates of barley seeds dipped in the NBs water and distilled water were 66% and 43% respectively. While after 50 hours, all the seeds in each group were germinated. Then, the amount of ROS generation inside barley seeds was further studied to explain the faster germination process caused by NBs.

The superoxide radical ($O_2^{\cdot-}$) were detected and quantified using the NBT staining method. ROS were visualized in seeds by NBT, which produced formazan within the seed cell at the sites of ROS formation (Fig. 7).

The generation of ROS in the germinating barley seed was very heterogeneous. The accumulation of ROS was observed mainly in the embryo part (data not shown). The microscope spectrophotometer gave the UV-visible spectra, and spectral analyses were done from small areas on the sample. The diameter of microscopic sample dot was 10 μm. For both the germinated seeds dipped in the water containing NBs and water without NBs, ROS were observed inside the seeds after 22hours dipping time. After 50 hours dipping time, the darkness of dark-blue compound in both the seeds dipped in the water containing NBs and water without NBs became lower (Fig. 7), which meant that the ROS levels in barley seeds decreased after 50 hours of dipping in the water.

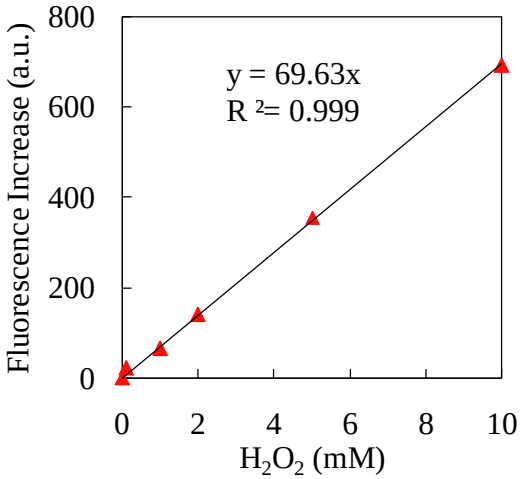

Fig. 6 Fluorescence increase of APF in H_2O_2 system. (The fluorescent intensity represents the oxidative capacity of H_2O_2; 1μM APF was added in the phosphate buffer (0.1M, pH 7.4). The fluorescence intensity was determined at 515nm with excitation at 490nm

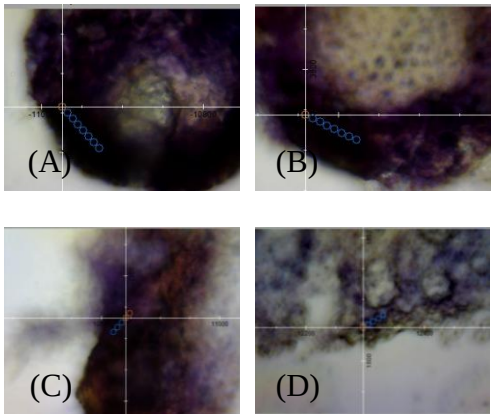

Fig. 7 Images of ROS produced after imbibitions in the sprout part of barley seeds. Dark blue staining indicates the ROS production. (A) and (C) were germinated with NBs water. (B) and (D) were germinated in the distilled water. (A) and (B) were 22 hours' dipping. (C) and (D) were 50 hours' dipping

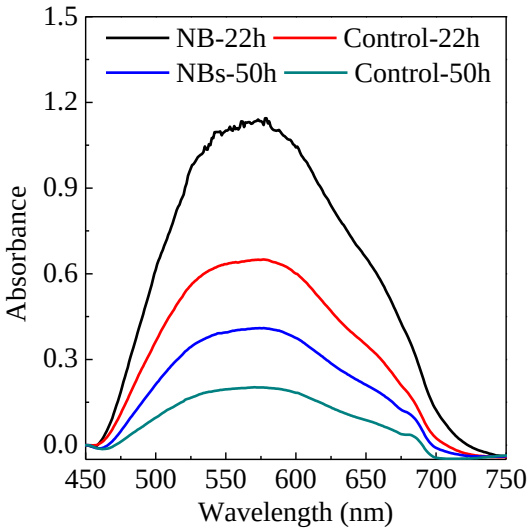

Fig. 8 Spectra of formazan formed as a result of ROS production in germinated barley seeds. For each group we measured 3 seeds. Each curve represents the mean value of more than 100 microscopic sample dots

The quantification of ROS inside seeds was achieved with the spectra of microscopic samples. ROS (superoxide radical $O_2^{\cdot}$) reduced the yellow dye (NBT) to a blue-colored formazan, which was measured spectrophotometrically at 560 nm. For each sample, 5-12 dots were selected according to the darkness of color. And the average absorbance values were calculated to compare the amount of ROS in the seeds dipped in the water with and without NBs. As can be seen in Fig. 8, the absorbance value around 560 nm of seeds germinating in the water containing NBs were obviously larger than those in the water without NBs at the same dipping time.

The DO concentrations of NBs water and the water without NBs were adjusted to be the same. Thus, the increase of ROS was caused only by the NBs themselves, although the ROS generated by NBs was in vitro. Exogenously supplied H_2O_2 can promote the germination of cereal plants, such as barley, wheat, rice and zinnia elegans seeds as well (Naredo et al. 1998; Ogawa K and Iwabuchi M 2001). As a result, the ROS generated by NBs would also promote the germination process of barley seed.

The appropriate amount of ROS can promote the growth of plant. However, overproduction of ROS may also have negative effects. The results will play a guiding role for the application of NBs technology in the agriculture field.

4 Conclusions

In summary, we provide the direct evidence that oxygen NBs can generate ROS in the water. The oxidative capacity of 60 minutes generation of oxygen NBs was higher than 0.85μM $\dot{O}H$ or 1.5 mM H_2O_2. The seeds dipped in the water containing NBs could generate more ROS compared to those in the distilled water. These constitute a novel mechanism for NBs' promotion effect on physiological activity of living organisms. Once fully understanding NBs' effect on living organism growth is achieved, the manipulation of NBs will develop a new technology in agricultural applications.

Acknowledgements

A part of this research was financially supported by the Challenging Exploratory Research (25660202) and the Grant in Aid for Scientific Research (24･02408) by JSPS and Fine Bubble Project (SIP, Japan). The nanoparticle tracking analysis data was technically supported by Ms. Ayako Irie at Quantum Design Inc., Japan.

Reference

Ago, K., Kazuo, N., Jun, T., Ruriko, I., Naoya, M., Kiichi, M., Koji, T., 2005. Development of an aerobic cultivation system by using a microbubble aeration technology. J Chem. Eng. Jap. 38(.9), 757-762

Agrwal, A., Xu, H., Ng, W.J., Liu, Y., 2012, Biofilm detachment by self-collapsing air microbubbles: a potential chemical-free cleaning technology for membrane biofouling. J. Mater. Chem. 22, 2203-2207.

Chen, X.J., West, A.C., Cropek, D.M., Banta S. 2008. Detection of the Superoxide Radical Anion Using Various Alkanethiol Monolayers and Immobilized Cytochrome c Anal. Chem. 80, 9622–9629.

Chu, L.B., Yan, S.T., Xing, X.H., Yu, A.F., Sun, X.L., Jurcik, B., 2008. Enhanced sludge solubilization by microbubble ozonation. Chemosphere 72, 205–212

Donghue, M.A., Xu, X., Bernlohr, D.A., Arriaga, E.A., 2013. Capillary electrophoretic

analysis of hydroxyl radicals produced by respiring mitochondria. Anal. Bioanal. Chem. 405, 6053-6060.

Ebina, K., Shi, K., Hirao, M., Hashimoto, J., Kawato, Y., Kaneshito, S., Morimoto, T., Koizumi, K., Yoshikawa, H., 2013. Oxygen and air nanobubble water solution promote the growth of plants, fishes, and mice. PLoS ONE 8, 1-7

Hiroyuki, A., Kenji, A., Masato, F., Fumio, T., Katsuine, T., Yoshihisa, N., 2010. Study on cleaning of pipe inner wall by microbubble flow. Japanese J. Multiphase Flow. 24(4), 454-461

Ikeura, H., Kobayashi, F., Tamaki, M. 2011. Removal of residual pesticides in vegetables using ozone microbubbles. J. Hazard. Mater. 186(1), 956-959.

Ishibashi, Y., Tawaratsumida, T., Zheng, S.H., Yuasa, T., Mari, Iwaya-Inoue. 2010. NADPH Oxidases act as key enzyme on germination and seeding growth in barley (*Hordeum vulgare* L.). Plant Prod. Sci. 13(1), 45-52

Kopechek,J.A., Haworth, K.J., Radhakrishnan, K., Huang, S.L., Klegerman, M.E., McPherson, D.D., Holland, C.K., 2013. The impact of bubbles on measurement of drug release from echogenic liposomes. Ultrasonics Sonochemistry 20, 1121–1130

Kurata, K., Taniguchi, H., Fukunaga, T., Matsuda, J., Higaki, H., 2007. Development of a Compact Microbubble generator and its usefulness for three dimensinal osteoblastic cell culture. Journal of Biomechanical Science and Engineering, 2(4), 166-177

Lakowica, J.R., Weber, G., 1973. Quenching of fluorescence by oxygen. A probe for structural fluctuations in macromolecules. Biochemical 12(21), 4161-4170.

Lakowicz,J.R.,2010.Principlesof fluorescence spectroscopy 3rd edition. Springer, pp 278.

Li, P., Takahashi, M., Chiba, K., 2009. Enhanced free-radical generation by shrinking microbubbles using a copper catalyst. Chemosphere. 77, 1157-1160.

Liu, S., Kawagoe, Y., Makino, Y., Oshita, S., 2013. Effects of nanobubbles on the physicochemical properties of water: the basis for peculiar properties of water containing nanobubbles. Chem. Eng. Sci. 93, 250-256.

Liu, S., Wang, Q.H., Sun, T.C., Wu, C.F., Shi, Y. 2012. The effect of different types of micro-bubbles on the performance of the coagulation flotation process for coke waste-water. J Chem Technol Biotechnol 82 (2), 206–215

Mabuchi, T. 1994. Studies on the dormancy-awakening and breaking in the two-bowed barley seed. Jpn. J. Crop Sci. 63: 436-441.

Margaret, A., Donogue, Xu, X., Bernloht, D.A., Arriaga, E.A., 2013. Capillary electrophoretic analysis of hydroxyl radicals produced by respiring mitochondria. Ana Bioanal Chem. 405, 6053-6060.

Muller, K., Linkies, A., Vreeburg, R.A.M., Fry, S.C., Krieger-Liszkay, A., Leubner-Metzger, G. 2009. In vivo cell wall loosening by hydroxyl radicals during cress seed germination and elongation growth. Plant Physiol. 150, 1855-1865.

Najafi, A.S., Drelich, J., Yeung, A., Xu, Z., Masliyah, J., 2007. A novel method of measuring electrophoretic mobility of gas bubbles. J Colloid Interface Sci, 308, 344-350.

Naredo, M.E.B., Juliano, A.B., Lu, B.R., de Guzman, F., Jackson, M.T., 1998. Responses to seed dormancy-breaking treatments in rice species (*Oryza L.*). Seed Sci. Technol. 26, 675-689.

Ogawa, K., Iwabuchi, M., 2001. A mechanism for promoting the germination of Zinnia elegans seeds by hydrogen peroxide. Plant Cell Physiol. 42(3), 286-291

Park, J.S., Kenji, K., 2009. Application of microbubbles to hydroponics solution promotes lettuce growth. Horttechnology, 19, 212-215

Passardi, F., Penel, C., Dunand, C., 2004. Performing the paradoxical: how plant peroxidases modify the cell wall. Trends Plant Sci 9:534 – 540

Seddon, J.R.T., Lohse, D., Craig, V.S.J., 2012. A deliberation on nanobubbles at surfaces and in bulk. ChemPhysChem 13, 2179-2187.

Setsukinai, Ken-ichi., Urano, Y., Kakinuma, K., Majima, H.J., Nagano, T., 2003. Development of nocel fluorescence probes that can reliably detect reactive oxygen species and distinguish specific species. J. Biol. Chem. 278(5), 3170-3175.

Takahashi, M., Chiba, K., Li, P., 2007. Formation of hydroxyl radicals by collapsing ozone microbubbles under strongly acidic conditions. J. Phys. Chem. B. 111, 11443-11446.

Takahashi, M., Ishikawa, H., Asano, T., Horibe, H., 2012. Effect of microbubbles on ozonized water for photoresist removal. J. Phys. Chem. C. 116, 12578-12583.

Tomizama, S., Imai, H, Tsukada, S., Simizu, T. 2005. The detection and quantification of highly reactive oxygen species using the novel HPF fluorescence probe in a rat model of focal cerebral ischemia. Neuoscience Research 53, 304-313.

Xiaojun J. Chen, Alan C. West, Donald M. Cropek, Scott Banta. 2008. Detection of the Superoxide Radical Anion Using Various Alkanethiol Monolayers and Immobilized Cytochrome c. Anal. Chem. 80, 9622–9629